Discrete infinity harmonic functions: towards a unified interpolation framework on graphs

Mahmoud Ghoniem, Abderrahim Elmoataz, Olivier Lezoray

DISCRETE INFINITY HARMONIC FUNCTIONS: TOWARDS A UNIFIED INTERPOLATION FRAMEWORK ON GRAPHS

Mahmoud Ghoniem, Abderrahim Elmoataz, Olivier Lezoray

GREYC, université de Caen Basse-Normandie

ABSTRACT

In this paper, we introduce fast and robust digital algorithms for solving the Dirichlet problem with ∞-harmonic functions on graphs. Several PDEs and variational techniques have been proposed for a number of interpolation problems. Our motivation for this work is to extend some of these PDEs on graphs to deal with interpolation problems with a new approach in a discrete framework using the ∞-Laplacian on weighted graphs arbitrary topology. We show the experimental results for some applications of image interpolation that demonstrate the efficiency of our method and point out the interest of the novel algorithm with $p = \infty$ for interpolation problems.

Index Terms— ∞-harmonic functions, interpolation, inpainting, semi-supervised segmentation, ∞-Laplacian

1. INTRODUCTION

Many tasks in image processing and computer vision can be formulated as interpolation problems. Image and video colorization, inpainting and semi-supervised segmentation are examples of these problems. In general, interpolating data consists in constructing new values for missing data in coherence with a set of known data. In recent years, many methods have been developed for image interpolation. Among them, a number of methods are based on Partial Differential Equation (PDE) or variational. They have shown their efficiency in giving an approximation of the missing data.

Let us consider a function f defined on a continuous euclidean domain Ω and $A \subseteq \Omega$ represents missing data. One of the simplest way is to approach $f|_A$ by the p-harmonic function on A, having the Dirichlet boundary data $f|_{\Omega\backslash A}$ on $\Omega\backslash A$. Mathematically, interpolating f over A is formalized as:

$$\begin{cases} \lim\limits_{p\to\infty} \frac{1}{p} \int |\nabla f|^p \, \mathrm{d}x = 0 & \text{on } A \\ f = g & \text{on } \partial A = \Omega\backslash A \end{cases}$$

Equation (1) can be solved by considering the p-Laplacian equation:

$$\begin{cases} \Delta_p f = 0 & \text{on } A \\ f = g & \text{on } \partial A \end{cases} \tag{1}$$

For $p = 2$, we retrieve harmonic function and when $p \to \infty$, we obtain the ∞-harmonic functions that are widely used for data interpolation in continuous domains [1, 2].

However, these methods are local, hence, they are not adapted for interpolating images containing texture. That explains the interest in the methods that exploit nonlocal information based on patch similarity. For instance, some works utilize the non-parametric sampling of Efros and Leung [3] and explore the self-similarity in the image or video to regularize the preserved data [4, 5].

Hence, recent works tend to unify the local and nonlocal interpolation approaches [6]. A variational framework for nonlocal image inpainting has been presented [7]. A discrete nonlocal regularization framework for image and manifold processing has been proposed [8]. This framework has been used to present a unifying approach of local geometric methods and nonlocal exemplar-based ones for video inpainting [9, 10].

This paper addresses the problem of data interpolation on weighted graphs of arbitrary topology and demonstrates some applications of image interpolation. Our main contribution lies in providing a new method for solving the Dirichlet problem with ∞-harmonic functions on graphs of arbitrary topology. This method provides simple and fast algorithms for image interpolation and inpainting. A main advantage of our approach is the unification of local and nonlocal approaches for these processing procedures in a mathematically unified discrete framework which makes it applicable to any data represented on graphs. Our new algorithm, with $p = \infty$, provides competing results but is computationally much faster than other values of $p < \infty$.

In Section 2, we state the interpolation issue in terms of Dirichlet problem on graphs. In Section 3, we report and discuss empirical results of our proposed methods for image and video inpainting. We conclude this paper in Section 4 with a summary of our findings.

2. ∞-HARMONIC INTERPOLATION ON GRAPHS

We consider that data are defined on a general domain represented on a graph $G = (V, E, w)$. Let $f : V \to \mathbb{R}$ in

$\mathcal{H}(V)$ be a function. Let $A \subset V$ be the subset of vertices to interpolate and ∂A its external boundary with known data. Consequently, $V \setminus A$ corresponds to the known vertices.

Mathematically, interpolation problems using p-harmonic functions consist in finding a function f that minimizes the p-energy with given boundary conditions (specific values on ∂A).
For $1 \leq p < \infty$, the p-energy formula is:

$$\mathcal{R}_w^p(f) = \sum_{u \sim v} \|\nabla_w f(u)\|_p^p,$$

where $\nabla_w f(u)$ is the gradient as defined below.
Interpolating an image using ∞-harmonic functions consists in finding a function f that is the limit of p-harmonic functions: $f_p \xrightarrow[p \to \infty]{} f$ as described below.

2.1. Difference operators on graphs

Firstly, let us give the required definitions. We refer the reader to [8] for detailed definitions of derivatives on graphs.

The *gradient operator* of a function $f : V \to \mathbb{R}$, at a vertex $u \in V$, is the vector operator defined by:

$$\nabla_w f(u) = (\partial_v f(u) : v \sim u)^T = (\partial_{v_1} f(u), \ldots, \partial_{v_k} f(u))^T, \tag{2}$$

where $v_1, \ldots, v_k$ are the neighbors of the vertex u.

The *anisotropic p-Laplace* operator $\Delta_{p,w} : \mathcal{H}(V) \to \mathcal{H}(V)$, of a function $f : V \to \mathbb{R}$, at a vertex $u \in V$ is:

$$\Delta_{p,w} f(u) = \sum_{v \sim u} w(u,v)^{\frac{p}{2}} |f(u) - f(v)|^{p-2} (f(u) - f(v)) \tag{3}$$

The *upwind gradients* are defined by:

$$\begin{aligned} \|\nabla_w^- f(u)\|_\infty &= \max_{v \sim u} \left(\sqrt{w(u,v)} \max (f(u) - f(v), 0) \right) \quad (4) \\ \|\nabla_w^+ f(u)\|_\infty &= \max_{v \sim u} \left(\sqrt{w(u,v)} \max (f(v) - f(u), 0) \right) \end{aligned}$$

The definition of the ∞-*Laplacian*, $\Delta_{\infty,w}$, is written:

$$(\Delta_{\infty,w} f)(u) = \|\nabla_w^- f(u))\|_\infty - \|\nabla_w^+ f(u)\|_\infty. \tag{5}$$

Using the gradients definitions, the ∞-Laplacian becomes:

$$(\Delta_{\infty,w} f)(u) = \frac{2\, f(u) - (\max_{v \sim u} (f(v)) + \min_{v \sim u} (f(v)))}{2} \tag{6}$$

Thus, we obtain the expression of the morphological Laplacian which is an approximation of the continuous ∞-Laplacian.

2.2. ∞-harmonic functions

Definition 1. A function f is ∞-*harmonic* iff:

$$f(u) = \lim_{p \to \infty} f_p(u), \quad \forall u \in A \backslash \partial A \tag{7}$$

where f_p is a p-harmonic function, i.e. that satisfies:
$\Delta_p f_p(u) = 0$.

Proposition 1. A function f is ∞-harmonic iff

$$f(u) = \frac{2\, f(u) + |(\nabla_w^+ f)(u)|_\infty - |(\nabla_w^- f)(u)|_\infty}{2} \tag{8}$$

Or equivalently, $\Delta_{\infty,w} f = 0$.

To get its solution, several methods can be used. By solving the fixed point iteration we obtain the following algorithm.
$\forall (u,v)$ with u and v in A:

$$\begin{aligned} f^{(0)}(u) &= f^0(u), \quad \forall u \in A \\ f^{(k)}(u) &= f^0(u), \quad \forall u \in \partial A \\ f^{(k+1)}(u) &= f^{(k)}(u) \quad \forall v \in A \\ &\quad + \left(\max_{v \sim u} \left(\sqrt{w(u,v)} \max (f(u) - f(v), 0) \right) \right) \setminus 2 \\ &\quad + \left(\max_{v \sim u} \left(\sqrt{w(u,v)} \max (f(v) - f(u), 0) \right) \right) \setminus 2, \end{aligned} \tag{9}$$

More inquisitive readers are referred to [11] for more details on ∞-harmonic functions on graphs and for the existence and uniqueness of a solution of Equation (8) and the convergence of Equation (9) to Equation (8).

3. EXPERIMENTAL RESULTS

3.1. Graph construction

First of all, the graph is constructed. The weight function w associated to G provides a measure of the distance between its vertices that can simply incorporate local, semi-local or nonlocal features according to the topology of the graph and the image. Hence, our ∞-Laplacian can be either local or nonlocal depending on the use of w_L or w_{NL}.
We consider the following nonlocal weight function:

$$w_L(u,v) = exp\left(-\frac{|f(u) - f(v)|^2}{2\sigma_d^2} \right)$$

$$w_{NL}(u,v) = w_L(u,v).exp\left(-\frac{\|F(f^0,u) - F(f^0,v)\|^2}{h^2} \right),$$

where σ_d^2 depends on the variations of $|f(u) - f(v)|$ over the graph.

In addition to the difference between values, $w_{NL}(u,v)$ includes a similarity estimation of the compared features by measuring a $\mathcal{L}^2$ distance between the patches around u and v. Once the graph is constructed, the minimization problem is considered.

The iterative algorithm (9) is iterated till convergence is reached. We consider that convergence is reached when the Mean Squared Error between f^{k+1} and f^k is lower than a user-defined threshold.

3.2. Graph processing

3.2.1. Inpainting

It consists in filling in the missing parts of an image or a video with the most appropriate data in order to obtain harmonious and hardly detectable reconstructed zones.

(a) Corrupted image (b) $p = 2$ (c) $p = \infty$

Fig. 1. Comparison between the inpainting results using $p = 2$ and $p = \infty$.

(a) Initial image (b) Masked image (c) Restored image

Fig. 2. Inpainting of a real-life color image with $p = \infty$, a search window of size 21×21 and a patch of size 11×11.

In Figure 1, we can observe that the result with $p = \infty$ is similar to the inpainting with $p = 2$. We can remark that the case $p = 2$ can be interpreted as an iterative inpainting method based on the well-known nonlocal-means filter. In Figure 2, the security fencing has been removed to enjoy the zoo picture. The result on a texture image is reported in Figure 3. We can observe that the reconstructed zones are not detectable and merge harmoniously with the preserved data in both results with $p = 2$ and $p = \infty$.

We would like to stress that this equally good result is obtained at a much lower computational cost with $p = \infty$. In fact, by definition, the algorithm with $p = \infty$ is based on $max()$ functions while with p in $[1, \infty[$, it is based on weighted mean. Therefore, for the same number of iterations, the processing time is shorter for $p = \infty$ than $p = 2$ while giving equally competitive results. We notice that the algorithm with $p = 1$ is even slower than $p = 2$.

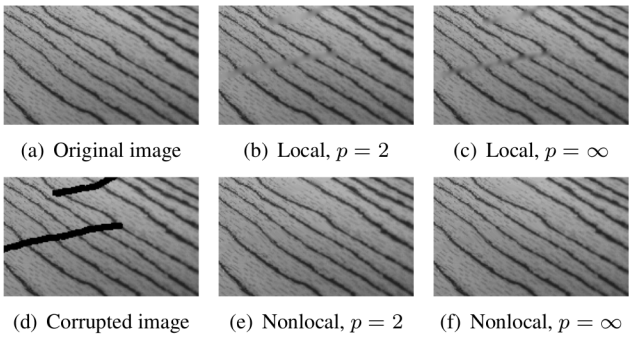

(a) Original image (b) Local, $p = 2$ (c) Local, $p = \infty$

(d) Corrupted image (e) Nonlocal, $p = 2$ (f) Nonlocal, $p = \infty$

Fig. 3. Inpainting of a texture image using a search window of size 31×31 and a patch of size 15×15.

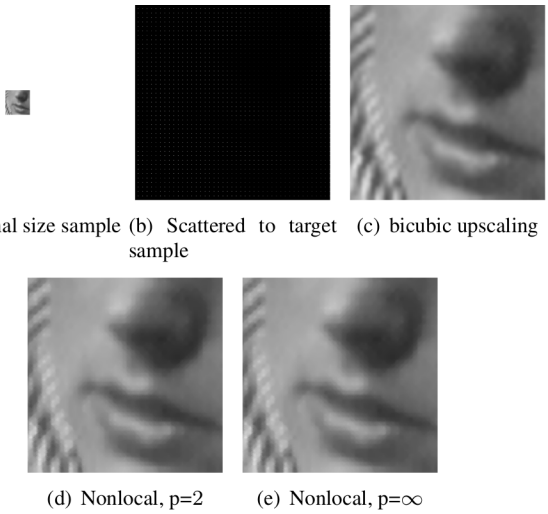

(a) Original size sample (b) Scattered to target sample (c) bicubic upscaling

(d) Nonlocal, p=2 (e) Nonlocal, p=∞

Fig. 4. Upscaling an image of Barbara. On the first line, from left to right, the region to enlarge, the same image scattered over the upscaled size and the bicubic upscaling. On the second line, from left to right, our nonlocal result for $p = 2$ and $p = \infty$.

Moreover, our experiments reveal that under the same convergence conditions, $p = \infty$ needs less iterations than $p = 2$ and much less than $p = 1$ to reach convergence. To sum up, $p = \infty$ has higher computation and convergence speeds than any other value of p for little or no visual difference. Hence, the real progress using $p = \infty$ resides in computational savings.

3.2.2. Upscaling

It consists in enlarging an initial image by constructing a big image from a low resolution content by adding new pixels with judicious values between the copied few original ones. This method has obvious direct application to image compression. Figure 4 shows the image of Barbara enlarged eight times while preserving texture and clear-cut edges. In comparison with bicubic upscaling, we can observe that our result is very similar but is less smoothed.

3.2.3. Semi-supervised segmentation

In this subsection we present the application of our method to semi-supervised segmentation. The semi-supervised segmentation provides a segmentation of data in two clusters given initial seeds. A user sets initial labels as shown in Figures 5 and 6 in order to obtain a segmentation of a target zone of his choice. Then, these initial labels are interpolated to similar regions all over the image using weights computed from the image to segment. At convergence of this process, the image is partitioned into two labels. In Figure 5 and 6 the boundary between the segmented regions is marked in red. This application can be used in an image and video matting algorithms.

4. CONCLUSION

In this paper, fast and robust digital algorithms for solving the Dirichlet problem with ∞-harmonic functions on graphs of arbitrary topology and some applications on image have been introduced. Besides the unification of state-of-the-art methods, the formulation with $p = \infty$ on graphs is novel and leads to a faster algorithm than classical approaches as aforementioned.

Experimental results on several interpolation applications demonstrate the efficiency of our algorithm for dealing with both image geometry and texture. Image inpainting and upscaling tests provide hardly detectable reconstructed data and semi-supervised segmentation tests were successful in segmenting different labeled textures.

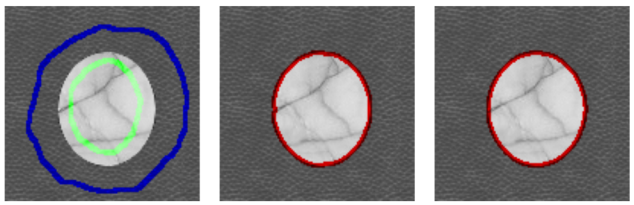

(a) Initial labels (b) $p = 2$ (c) $p = \infty$

Fig. 5. From left to right: An image of leather and marble texture with initial user-defined labels marking the target region and the background, the segmentation results for $p = 2$ and for $p = \infty$.

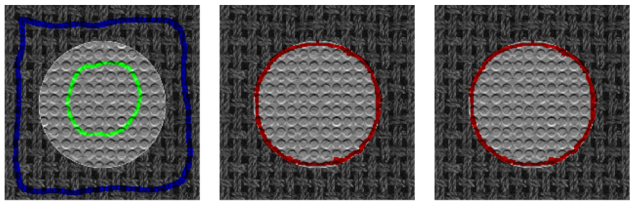

(a) Initial labels (b) $p = 2$ (c) $p = \infty$

Fig. 6. From left to right: An image of two different textures with initial user-defined labels, the segmentation results for $p = 2$ and for $p = \infty$.

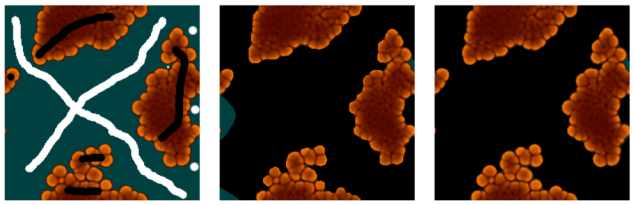

(a) Initial labels (b) $p = 2$, 1004 iterations (c) $p = \infty$, 391 iterations

Fig. 7. Matting example on *algae* image. With $p = \infty$, the algorithm is much faster (see number of iterations at convergence) than with $p = 2$ and provides a better result.

5. REFERENCES

[1] V. Caselles, J-M. Morel, and C. Sbert, "An axiomatic approach to image interpolation," *IEEE Transactions on Image Processing*, vol. 7, no. 3, pp. 376–386, 1998.

[2] L. Guillot and C. Le Guyader, "Extrapolation of vector fields using the infinity laplacian and with applications to image segmentation," in *SSVM*, 2009, pp. 87–99.

[3] A. Efros and T. Leung, "Texture synthesis by non-parametric sampling," in *IEEE International Conference on Computer Vision*, Corfu, Greece, September 1999, pp. 1033–1038.

[4] M. Bertalmio, L. Vese, G. Sapiro, and S. Osher, "Simultaneous structure and texture image inpainting," *IEEE Transactions on Image Processing*, pp. 882–889, 2003.

[5] A. Criminisi, P. Perez, and K. Toyama, "Region filling and object removal by exemplar-based image inpainting," *Image Processing, IEEE Transactions on*, pp. 1200–1212, 2004.

[6] G. Gilboa and S. Osher, "Nonlocal linear image regularization and supervised segmentation," *Multiscale Modeling & Simulation*, pp. 595–630, 2007.

[7] P. Arias, V. Caselles, and G. Sapiro, "A variational framework for non-local image inpainting," in *EMMCVPR09*, 2009, pp. 345–358.

[8] A. Elmoataz, O. Lezoray, and S. Bougleux, "Nonlocal discrete regularization on weighted graphs: a framework for image and manifold processing," *IEEE Transactions on Image Processing*, vol. 17, no. 7, pp. 1047–1060, 2008.

[9] M. Ghoniem, Y. Chahir, and A. Elmoataz, "Geometric and texture inpainting based on discrete regularization on graphs," in *ICIP*, 2009, pp. 1349–1352.

[10] M. Ghoniem, Y. Chahir, and A. Elmoataz, "Nonlocal video denoising, simplification and inpainting using discrete regularization on graphs," *Signal Processing*, vol. 90, no. 8, pp. 2445–2455, 2010.

[11] A. Elmoataz, M. Ghoniem, O. Lézoray, and V.T. Ta, "Nonlocal infinity laplacian on graphs with applications to image and data processing," *preprint*, 2011, Submitted.